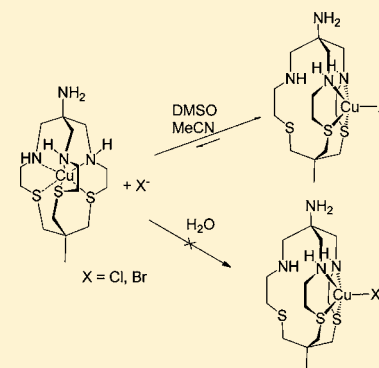


## Reversible Rearrangements of Cu(II) Cage Complexes: Solvent and Anion Influences

Paul V. Bernhardt,<sup>\*,†</sup> Helena Font,<sup>‡</sup> Carlos Gallego,<sup>‡</sup> Manuel Martínez,<sup>\*,‡</sup> and Carlos Rodríguez<sup>‡</sup><sup>†</sup>School of Chemistry and Molecular Biosciences, University of Queensland, Brisbane 4072, Australia<sup>‡</sup>Departament de Química Inorgànica, Facultat de Química, Universitat de Barcelona, Martí i Franquès 1-11, E-08028 Barcelona, Spain

## Supporting Information

**ABSTRACT:** The macrobicyclic mixed donor cage ligand AMME-N<sub>3</sub>S<sub>3</sub>sar (1-methyl-8-amino-3,13,16-trithia-6,10,19-triazabicyclo[6.6.6]eicosane) is capable of binding to Cu(II) as either a hexadentate (N<sub>3</sub>S<sub>3</sub>) or tetradentate (N<sub>2</sub>S<sub>2</sub>) ligand. The “Cu-in” (hexadentate)/“Cu-out” (tetradentate) equilibrium for the {Cu(AMME-N<sub>3</sub>S<sub>3</sub>sar)}<sup>2+</sup> units is strongly influenced by both solvent (DMSO, MeCN, and water) and halide ions (Br<sup>−</sup> and Cl<sup>−</sup>). We have established a crucial role of the solvent in these processes through the formation of intermediate solvato complexes, which are substituted by incoming halide ions triggering a final isomerization reaction. Surprisingly, for reactions carried out in the usually strongly coordinating solvent water, the completely encapsulated N<sub>3</sub>S<sub>3</sub>-bound “Cu-in” form is dominant. Furthermore, the small amounts of the “Cu-out” form present in equilibrated DMSO or MeCN solutions revert entirely to the “Cu-in” form in aqueous media, thus preventing reaction with halide anions which otherwise lead to partial or even complete decomposition of the complex. From the kinetic, electrochemical, and EPR results, the existence of an outer-sphere H-bonded network of water molecules interacting with the complex inhibits egress of the Cu(II) ion from the cage ligand. This is extremely relevant in view of outer sphere interactions present in strongly hydrogen bonding solvents and their effects on Cu(II) complexation.



## INTRODUCTION

Multidentate, including macrocyclic, ligands are dominant in classical coordination chemistry due to the enhanced thermodynamic stability of their complexes and their kinetic resistance to dissociation relative to monodentate ligands. The hexadentate sarcophagine (sar, Chart 1) cages encapsulate a variety of transition metals and render them inert to substitution, regardless of the inherent ligand exchange rates of the metal. This has enabled kinetic and mechanistic studies of ligand exchange reactions on metal ions even as labile as Cu(II)<sup>1</sup> and Hg(II)<sup>2</sup> to be undertaken.

In complexes from the sar family the metal is usually completely encapsulated by the hexadentate coordinated cage ligand (bearing either an N<sub>6</sub> or N<sub>3</sub>S<sub>3</sub> donor set, Chart 1),<sup>3,4</sup> and removal of the metal from its cage is very difficult. Indeed, *direct* removal of classically inert metals such as Co(III) from the cage has not been reported. Reduction to the more labile Co(II) oxidation state is necessary, but even then demetalation requires extreme reaction conditions, such as concentrated acid or extraction of the metal with highly competitive ligands such as cyanide.<sup>5,6</sup>

The inherent difficulty in metal ion removal from these cages presents opportunities in the study of ligand substitution reactions on systems that would normally be too rapid to observe, even under rapid mixing (stopped flow) conditions. For example monodentate ligand/solvent exchange reactions

on Cu(II) are exceptionally rapid (diffusion controlled) so mechanistic studies of these reactions are challenging.<sup>7,8</sup>

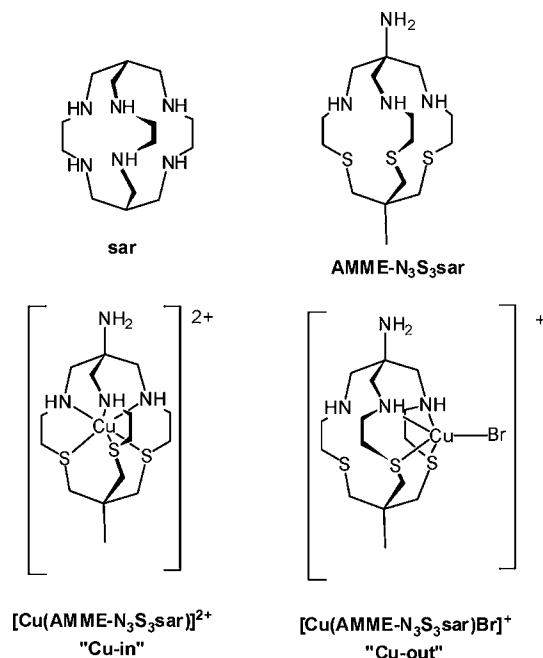
Cu(II) has exhibited a wide variety of coordination geometries in complexes with cage ligands with hexadentate (“Cu-in”),<sup>1,9–12</sup> pentadentate,<sup>10,12</sup> and tetradentate-coordinated (“Cu-out”)<sup>1,12,13</sup> ligands prepared and characterized crystallographically. Studies of Cu(II) complexes in these caged environments have a value-added perspective in view of their current development in positron emission tomography (PET) biomedical imaging using the positron emitting <sup>64</sup>Cu radio-nuclide,<sup>14</sup> where stability of the Cu(II) cage complex (covalently attached to an antibody) is crucial.

We have been involved in the study of the formation and isomerization behavior of transition metal complexes of a diversity of centers and macrocyclic N- and S-donor ligands.<sup>15–19</sup> Our studies of the decomposition and formation reactions of pentadentate amine ligands with Cu(II) have also revealed unexpected medium-related reactivity, which can be relevant when Cu(II) complexes are used as radiopharmaceuticals.<sup>20</sup> The influence of the solvent and other competing ligands, such as halide ions, on the stability of the Cu(II) complex is fundamentally important. In a recent paper<sup>1</sup> we reported the facile bromide-driven rearrangement (in DMSO) of the encapsulated six-coordinate (“Cu-in”) complex [Cu-

Received: August 2, 2012

Published: November 1, 2012

Chart 1



(AMME- $N_3S_3sar$ ) $^{2+}$  (Chart 1) to give the square pyramidal bromido complex  $[Cu(AMME-N_3S_3sar)Br]^+$  where the Cu atom was perched ("Cu-out") on an exterior face of the tetradentate-coordinated cage (see Chart 1). Our results indicated that the equilibrium reaction was rather complex with possible intervention of the solvent; nevertheless, the full spectroscopic and structural characterization of the "Cu-out" square pyramidal  $[Cu(AMME-N_3S_3sar)Br]^+$  complex was achieved.<sup>1</sup>

In this Article, we extend these studies to other solvents and halide ions in order to understand the influence of the competing ligands on the structure of the Cu(II) complex in solution. Some stark contrasts in reactivity in aprotic versus protic solvents are found which have important implications for potential applications of these ligands.

## RESULTS AND DISCUSSION

The involvement of the solvent as a ligand, as well as competing anionic ligands, has been established in some of our studies on equilibrium reactions involving macrocyclic metal complexes, both labile and inert.<sup>15,20</sup> Significant effects have been reported when polarity<sup>21–23</sup> and H-bonding influences are considered.<sup>24–26</sup> With these data in hand, and in view of the interesting preliminary kinetic results obtained for the "Cu-in"/"Cu-out" equilibria for  $[Cu(cis-V-AMME-N_3S_3sar)]^{2+}$  in DMSO and in the presence of bromide ions,<sup>1</sup> we have pursued

a full mechanistic investigation of the system in different solvents and in the presence of other halide ions.

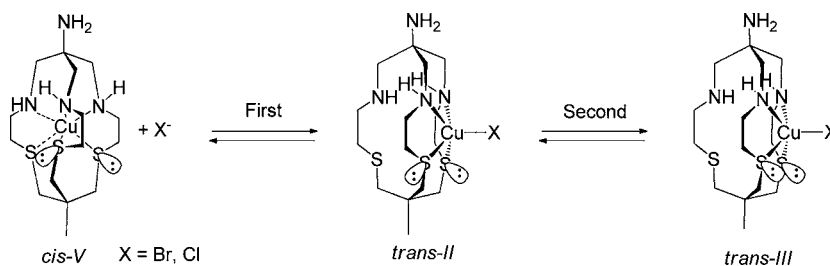
"Cu-in"/"Cu-out" Equilibria in DMSO and MeCN Solution. A detailed study of the stoichiometric reaction in Scheme 1 in DMSO and MeCN solutions was carried out at variable temperature and pressure as an extension of a previous study at 25 °C and ambient pressure (Figure 1) in DMSO solution. As shown in Scheme 1, N- and S-based isomerization reactions occur en route to the final product, and the nomenclature and the step-by-step processes have been described before and are maintained here.<sup>15,27</sup> Table 1 collects the results obtained using the techniques described in the Experimental Section. The spectral changes in all cases agree with the coalescence of the two charge-transfer bands of the initial octahedral complex in the 310–350 nm region, as well as the disappearance of the d–d transition at ca. 1300 nm, associated to the  $d_{z^2} \rightarrow d_{x^2-y^2}$  electronic transition, only apparent in tetragonally elongated 6-coordinate Cu(II) complexes.<sup>9</sup>

When the experiments were repeated using chloride as the incoming halido ligand, the results (also collected in Table 1) follow the same general trend observed for the reactions with bromide. Nevertheless, in this case the "Cu-out" species is unstable, and the reaction with chloride continues to give full decomposition of the complex with  $[CuCl_4]^{2-}$  and free AMME- $N_3S_3sar$  as the products, as evident from the pistachio color observed for the final solution (see below) and characteristic electronic spectrum of  $[CuCl_4]^{2-}$  in DMSO. Evidently, the higher stability of the Cu<sup>II</sup>–Cl bonds compared with Cu<sup>II</sup>–Br drives the reaction to full decomposition of the cage complex. From the data it is clear that the general behavior of the reactions in Scheme 1 are sensitive to the nature of the halide anion (or its derivative complexes). This is especially relevant for the process where no direct reaction with halide ions is observed (second step). Figure 2 summarizes these trends.

Given the differences observed, the use of another potentially inert solvent system was pursued. Thus, the reaction was also conducted and monitored in MeCN solution in the presence of bromide anions. The corresponding reaction with chloride ions in MeCN was not pursued due to the same instability of the  $[Cu(cis-V-AMME-N_3S_3sar)]^{2+}/Cl^-$  system identified first in DMSO (see above).

The reaction of  $[Cu(cis-V-AMME-N_3S_3sar)]^{2+}$  with bromide ions in MeCN revealed the same sequence of steps and trends seen in DMSO (Figures 1a,b and 2). The data, also collected in Table 1, clearly indicate that the second step (defined in Scheme 1), isomerization the *trans-II* bromido complex, is independent of solvent (Figure S1), as expected from the proposed mechanism. The process has a large activation enthalpy, while the values of  $\Delta S^\ddagger$  and  $\Delta V^\ddagger$  are close to zero. These data lead to the conclusion that the Cu–S bond breaks

Scheme 1



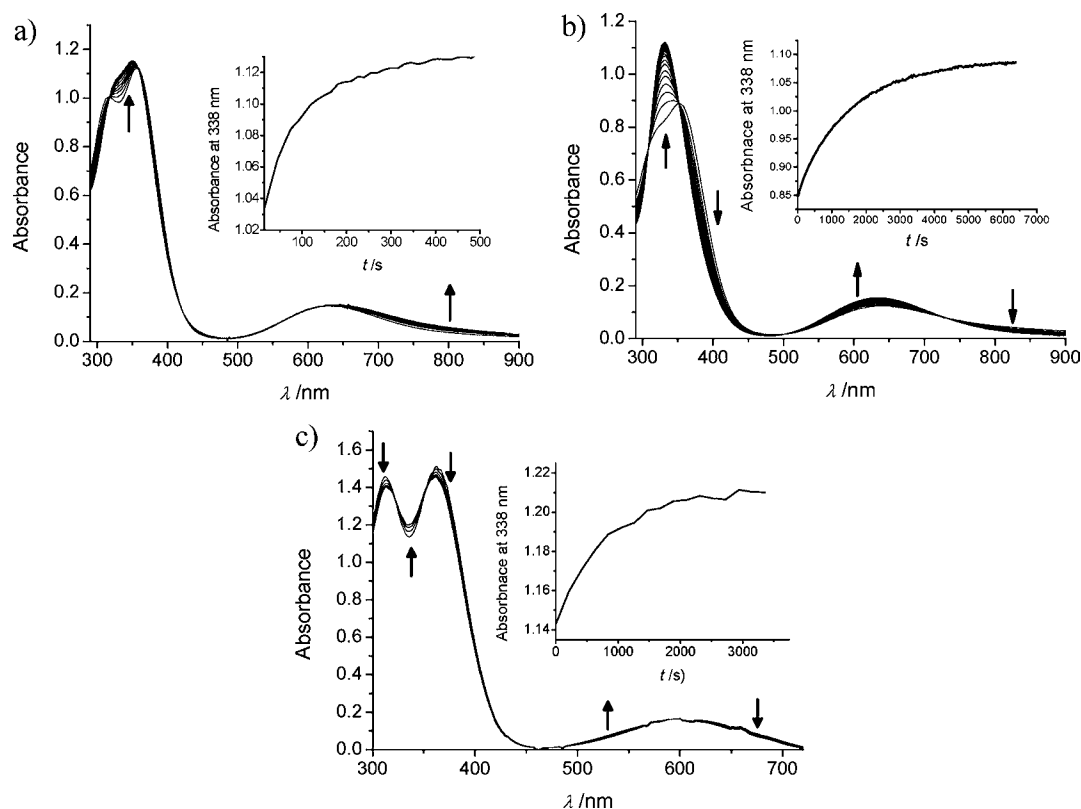


**Figure 1.** (a) Changes observed on the first fast step (Scheme 1) of the reaction of a ca.  $2 \times 10^{-4}$  M MeCN solution of  $[\text{Cu}(\text{cis-V-AMME-N}_3\text{S}_3\text{sar})](\text{ClO}_4)_2$  with 0.025 M  $(\text{Bu}_4\text{P})\text{Br}$  at 15 °C. (b) Changes observed on the slow second step (Scheme 1) of a ca.  $2 \times 10^{-4}$  M MeCN solution of the same complex with 0.10 M  $(\text{Bu}_4\text{P})\text{Br}$  at 35 °C. (c) UV-vis spectral changes observed on dilution of a  $1 \times 10^{-2}$  M DMSO solution of  $[\text{Cu}(\text{cis-V-AMME-N}_3\text{S}_3\text{sar})](\text{ClO}_4)_2$  in MeCN to a final ca.  $2 \times 10^{-4}$  M at 25 °C and 600 atm.

**Table 1. Summary of the Kinetic and Thermal and Pressure Activation Parameters Determined for the System Indicated in Scheme 1 in a Variety of Solvents and with Different Halide Ions**

solvent	halide	step	$10^3 \times {}^{298}k/\text{s}^{-1}$	$10^3 \times {}^{298}k/\text{M}^{-1} \text{s}^{-1}$	$\Delta H^\ddagger/\text{kJ mol}^{-1}$	$\Delta S^\ddagger/\text{J K}^{-1} \text{mol}^{-1}$	$\Delta V^\ddagger/\text{cm}^3 \text{mol}^{-1}$
MeCN	$\text{Br}^-$	first on	$[\text{X}^-]$ dependent	200	$57 \pm 3$	$-69 \pm 12$	$6 \pm 1$
MeCN	$\text{Br}^-$	first off	43		$68 \pm 7$	$-45 \pm 22$	$12 \pm 1$
MeCN	$\text{Br}^-$	second	0.28		equivalence with the data in DMSO solution, see Figure S1		<i>a</i>
DMSO	$\text{Br}^-$	first on <sup>1</sup>	$[\text{X}^-]$ dependent	83	$97 \pm 13$	$60 \pm 42$	$-16 \pm 4$
DMSO	$\text{Br}^-$	first off <sup>1</sup>	17		$55 \pm 4$	$-95 \pm 31$	$-35 \pm 5$
DMSO	$\text{Br}^-$	second <sup>1</sup>	0.30		$90 \pm 1$	$-11 \pm 5$	$-3 \pm 1$
DMSO	$\text{Cl}^-$	first on	$[\text{X}^-]$ dependent	3800	$47 \pm 4$	$-78 \pm 13$	<i>a</i>
DMSO	$\text{Cl}^-$	first off	83		$44 \pm 4$	$-120 \pm 15$	<i>a</i>
DMSO	$\text{Cl}^-$	second	29		$38 \pm 4$	$-166 \pm 12$	<i>a</i>
DMSO	none	<i>b</i>	1.6		$75 \pm 7$	$-20 \pm 24$	<i>c</i>
MeCN	none	<i>b</i>	1.1		$98 \pm 7$	$24 \pm 23$	$\sim 0$

<sup>a</sup>Not measured, complete decomposition of the complex occurs. <sup>b</sup>A single reaction is observed. <sup>c</sup>Not measured, DMSO freezes under the desired temperature/pressure conditions.

in the *trans-II* form to permit S-inversion and recoordination to generate the stable *trans-III* form. This is consistent with data obtained for thioether inversion processes studied on other macrocyclic ligand complexes with significant involvement of the competing ligands.<sup>15</sup> For the chlorido species the values determined in DMSO solution for  $\Delta H^\ddagger$  and  $\Delta S^\ddagger$  correspond to a much more associatively activated reaction (low values for  $\Delta H^\ddagger$  and very negative  $\Delta S^\ddagger$ ). The fact that the  $[\text{Cu}(\text{AMME-N}_3\text{S}_3\text{sar})\text{Cl}]^+$  intermediate (putatively formed) decomposes to  $[\text{CuCl}_4]^{2-}$ , implies the association of excess  $\text{Cl}^-$  leading to substitution of the S-donors upon breaking the Cu–S bonds

and then  $\text{Cl}^-$  replacement of the remaining N-donors (see below).

Although the data measured for the second step on the bromido complexes indicated in Scheme 1 are equivalent in both DMSO and MeCN, for the first step their corresponding values are disparate. For the reaction carried out in a solvent with higher affinity for copper (MeCN) a faster process is observed than for DMSO (Figure 2 and Table 1). The nonequivalence of the reaction rates obtained for the first step in Scheme 1 in different solvents thus must be related to a direct coordination of the solvent to Cu. Furthermore, these differences indicate that such an involvement is rate

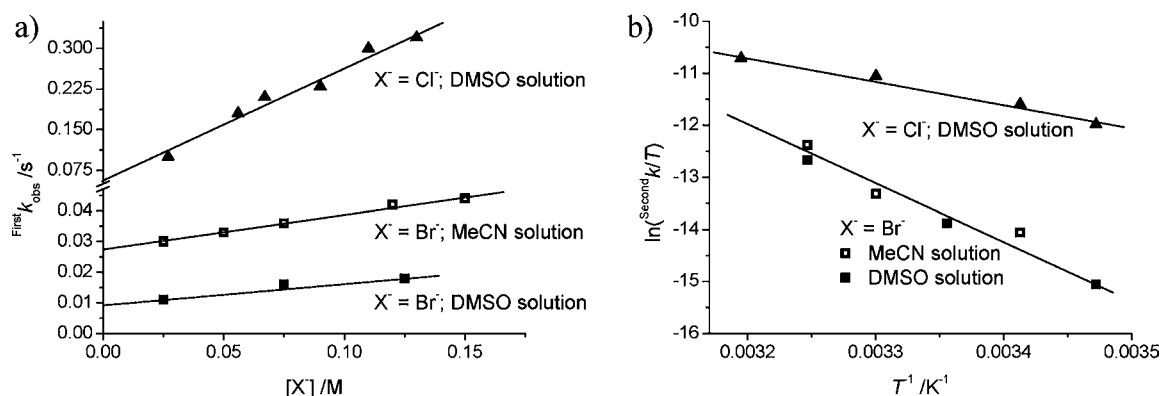
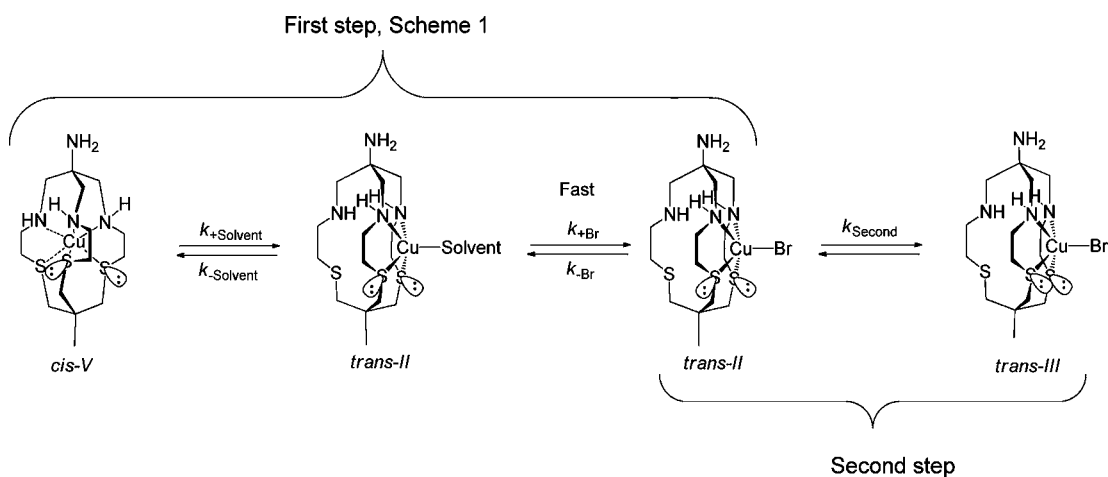


**Figure 2.** (a) Variation of the observed rate constants for the first step of the reaction of  $[\text{Cu}(\text{cis-V-AMME-N}_3\text{S}_3\text{sar})]^{2+}$  with halide anions in DMSO and MeCN solutions at 20 °C. (b) Eyring plots of the rate constants for the second step of the reaction for the same systems.

### Scheme 2



determining. The sequence indicated in Scheme 2 accommodates these mechanistic observations.

Consequently, the rate law expected for the first set of two reactions, when steady state conditions are applied to the *trans-II* solvato species, is indicated in eq 1.<sup>28</sup> If the  $k_{-\text{Solvent}}$  value is dominant in the disappearance of the intermediate solvato species, the equation becomes  $k_{\text{obs}} = k_{-\text{Br}} + (k_{+\text{Solvent}} \times k_{+\text{Br}} / k_{-\text{Solvent}})[\text{Br}^-]$ , in good agreement with the trends observed in Figure 2a with  $k_{\text{off}} = k_{-\text{Br}}$  and  $k_{\text{on}} = \{(k_{+}/k_{-})_{\text{Solvent}} \times k_{+\text{Br}}\}$ . This approximation fully agrees with a definitive influence of the solvent in the values of  $k_{\text{on}}$  and  $k_{\text{off}}$  determined for the systems studied. The activation parameters collected in Table 1 consequently correspond to the combination of the effects produced by bromide and solvent which makes their mechanistic interpretation impossible.

$$k_{\text{obs}} = \frac{k_{-\text{Solvent}}k_{-\text{Br}} + k_{+\text{Solvent}}k_{+\text{Br}}[\text{Br}^-]}{k_{-\text{Solvent}} + k_{+\text{Br}}[\text{Br}^-]} \quad (1)$$

In MeCN solution, the expansive ordering behavior, as found in water crystallization ( $\Delta V^\ddagger > 0$  and  $\Delta S^\ddagger < 0$ ), indicates that hydrogen-bonded interactions are dominant in the reaction;<sup>29–31</sup> in DMSO solution the data are less straightforward to interpret. Nevertheless, the bulkier nature of the solvent can be held responsible for the differences, provided the formation of the “Cu-out” complex, promoted by the solvent, becomes the dominant step in the overall process in this medium. If this is so, for the on process, a more dissociative transition state is

expected with little participation of such a bulky ligand, even though hydrogen-bonding interactions with the N–H donors of the ligand are still expected. For the off reaction, the process should become much more associatively activated by participation of the encapsulating ligand, in accord with the microreversibility principle. That is, the increased dissociative-ness of the on process masks the hydrogen bonding dominant interactions for the reaction.

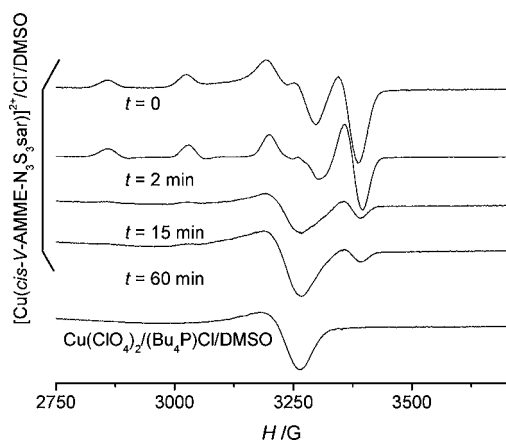
The reactivity of the “Cu-in”  $[\text{Cu}(\text{cis-V-AMME-N}_3\text{S}_3\text{sar})](\text{ClO}_4)_2$  complex in the neat solvents used for its reaction with halides was further pursued (i.e., the first reaction  $k_{\pm\text{Solvent}}$  in Scheme 2). Furthermore, both in DMSO and MeCN solution, the effective equilibrium constant for the first set of two reactions is ca. 5 (i.e.,  $k_{\text{on}}/k_{\text{off}}$ ), which might allow the detection of the solvato species indicated in Scheme 2 in absence of the final halide substitution reaction. This was achieved by dilution of concentrated stock samples of the complex in DMSO or MeCN into the same solvents, which led to monophasic changes in the UV–vis spectra. These changes are very small (only 2–6% of the absorbance values of the ligand to metal (S→Cu) charge transfer transitions at ca. 340 nm, Figure 1c) compared with those observed for the reaction with halide ions, and, in contrast to those,<sup>1</sup> do not lead to a coalescence of the two LMCT bands. Thus, the presence of finite amounts of  $[\text{Cu}(\text{trans-II-AMME-N}_3\text{S}_3\text{sar})(\text{Solvent})]^{2+}$  (Solvent = MeCN, DMSO) (Scheme 2) is proposed.



Table 1 collects the kinetic and thermal and pressure activation parameters measured for the single process observed in neat solvent (i.e., no halide ions added). Although the observed rate constants determined at room temperature are equivalent within error limits, the activation parameters indicate a significant difference between the reactions observed in DMSO or MeCN. The values determined correspond to a  $(k_{+\text{Solvent}} + k_{-\text{Solvent}})$  term derived from Scheme 2. While the activation entropies are very close to zero, as well as the activation volume determined in MeCN solution, the larger values found for  $\Delta H^\ddagger$  reflect the influence of the more strongly bound MeCN ligand principally in the reverse ( $k_{-\text{Solvent}}$ ) step. Nevertheless, as a whole, the activation data correspond to a mixture of dissociatively activated processes ( $k_{+\text{Solvent}} + k_{-\text{Solvent}}$ ), the first one being essentially common to both DMSO and MeCN.

From the data obtained it is clear that, in the absence of halide anions, the equilibrium position of the first reaction in Scheme 2 (in DMSO or MeCN) lies very much to the left. As indicated below, such a small displacement does not allow the isolation of the solvate-coordinated “Cu-out” intermediate in the absence of added halide anions.

For the reactions carried out in DMSO with a large excess of chloride, the final product is predominantly  $[\text{CuCl}_4]^{2-}$ . Examination of the UV–vis spectrum of the final reaction mixture shows a definite very intense peak at ca. 380 nm which is also produced by reaction of copper(II) perchlorate in DMSO solution with  $(\text{Bu}_4\text{P})\text{Cl}$ . Time resolved EPR experiments were also conducted to explore these reactions (Figure 3). The data indicate that, after the initial reaction producing a



**Figure 3.** EPR spectra (9.3966 GHz) of frozen  $1 \times 10^{-3}$  M DMSO solutions of  $[\text{Cu}(\text{cis-V-AMME-N}_3\text{S}_3\text{sar})](\text{ClO}_4)_2$  with  $[(\text{Bu}_4\text{P})\text{Cl}] = 0.1$  M run at different times after mixing. Comparison with the spectrum obtained on reaction with  $\text{Cu}(\text{ClO}_4)_2$  is also presented.

putative “Cu-out” chlorido complex, a further reaction takes place over the course of 1 h to generate a spectrum that is mostly due to  $[\text{CuCl}_4]^{2-}$  (see comparison with  $[\text{CuCl}_4]^{2-}$  at the bottom of Figure 3). A small amount of residual  $[\text{Cu}(\text{trans-III-AMME-N}_3\text{S}_3\text{sar})\text{Cl}]^+$  (peak at 3375 G) is seen at the end of the 60 min reaction period.

**“Cu-in”/“Cu-out” Equilibrium in Water.** In view of the important involvement of the solvent in the “Cu-in”/“Cu-out” rearrangement of  $[\text{Cu}(\text{cis-V-AMME-N}_3\text{S}_3\text{sar})]^{2+}$ , water, a coordinating solvent, was examined.<sup>32</sup> Dissolving solid  $[\text{Cu}(\text{cis-V-AMME-N}_3\text{S}_3\text{sar})](\text{ClO}_4)_2$  rapidly in water was found to be rather difficult; furthermore, the solution thus obtained was

found to retain its characteristic UV–vis–NIR spectrum for the *cis-V* hexacoordinated  $\text{N}_3\text{S}_3$  complex for hours at room temperature. The alternative dilution of a  $1 \times 10^{-2}$  M DMSO solution of  $[\text{Cu}(\text{cis-V-AMME-N}_3\text{S}_3\text{sar})](\text{ClO}_4)_2$  to a final  $2 \times 10^{-4}$  M concentration in water ( $\text{H}_2\text{O}:\text{DMSO}$  50:1) was conducted. Under these conditions neat monophasic spectral changes of  $\sim 5\text{--}10\%$  of the initial absorbance values were observed, but these (Figure 4a) were *opposite* to those observed for the halide reactions (see Figure 1). The observed first-order rate constant for the process was independent of pH within the range 2.9–5.0, although increasing steadily at higher pH values (Figure 4b). The reaction rate was also observed to be independent of copper concentration and the ionic strength (as for the other studies carried out). An increase of the DMSO content of the final solution, nevertheless, induces a definite decrease of the value determined for  $k_{\text{obs}}$  (Figure S2), thus indicating the importance of the solvent system in the process. The reactivity showed good reproducibility both at different temperatures and pressures. Table 2 collects the relevant kinetic and thermal and pressure activation parameters obtained for these processes with no halide added.

In order to ascertain that the reaction sequence in Scheme 2 is still valid in water, the reaction with halide anions was also conducted on the final water-equilibrated solutions at pH 3 and 9.7. Both for bromide and chloride anions the UV–vis spectral changes observed (Figure S3) indicated the formation of an equilibrium mixture of  $[\text{Cu}(\text{cis-V-AMME-N}_3\text{S}_3\text{sar})]^{2+}/[\text{Cu}(\text{trans-II-AMME-N}_3\text{S}_3\text{sar})(\text{X})]^+ / [\text{Cu}(\text{trans-III-AMME-N}_3\text{S}_3\text{sar})(\text{X})]^+$  is occurring although much more displaced to the initial  $[\text{Cu}(\text{cis-V-AMME-N}_3\text{S}_3\text{sar})]^{2+}$  form than in DMSO or MeCN media. That is, reliable and measurable absorbance changes were only obtained in these media when  $[\text{X}^-]$  was in the 0.5–3.0 M range. These changes (Figure 5a) showed monophasic behavior and lack of coalescence of the two charge-transfer bands at 310 and 380 nm, thus indicating that the process indicated in Scheme 2 is effectively limited to the first set of two reactions ( $k_{\text{Solvent}}$  plus  $k_{\text{Bromide}}$ ) in these cases. At pH = 3.0 the value of the first-order rate constants obtained from the spectral changes decreases on increasing the halide concentration as shown in Figure 5b. This trend fully agrees with eq 1 above, once the  $k_{+\text{Br}}[\text{X}^-]$  term becomes dominant versus  $k_{-\text{Solvent}}$  at very high halide concentration, with limiting values for  $k_{\text{obs}}$  being  $k_{+\text{Solvent}}$ . Table 2 also collects the relevant kinetic and activation parameters measured for the systems at  $[\text{X}^-] = 3$  M. From the data it is clear that  $k_{\text{obs}}$  is dominated by the neat  $k_{+\text{Solvent}}$  contribution at pH 3.0, as the value of the kinetic and thermal activation parameters is independent (within error limits) of the nature of the halide ion used involved in the process (Figure 6a). Nevertheless, at pH 9.7 this equivalence does not hold as seen in Figure 6b; the existence of  $K_{\text{a}}([\text{Cu}(\text{trans-II-AMME-N}_3\text{S}_3\text{sar})(\text{OH}_2)]^{2+}/[\text{Cu}(\text{trans-II-AMME-N}_3\text{S}_3\text{sar})(\text{OH})]^+)$  and the competition between possible  $k_{+\text{halide}}$  and  $k_{+\text{hydroxo}}$  terms in the reaction indicated in Scheme 2, is responsible for further complication of the system. It is clear that at pH = 3.0 the activation enthalpy supports the dissociatively activated character of the  $k_{+\text{Solvent}}$  contribution, although the values for  $\Delta S^\ddagger$  and  $\Delta V^\ddagger$  have a certain degree of association that can be related to the formation of hydrogen bonding networks found in other systems in similar aqueous medium (expansive ordering of hydrogen bonding networks).<sup>15,33,34</sup> The fact that the  $[\text{Cu}(\text{AMME-N}_3\text{S}_3\text{sar})]^{2+}$  complex has both NH and S

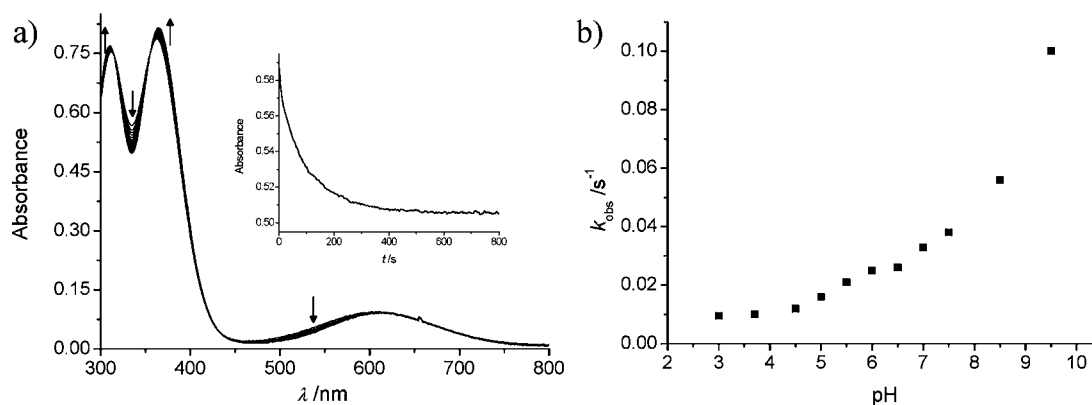


**Figure 4.** (a) UV-vis spectral changes observed on dilution of a  $1 \times 10^{-2}$  M DMSO solution of  $[\text{Cu}(\text{cis-V-AMME-N}_3\text{S}_3\text{sar})](\text{ClO}_4)_2$  in water at pH = 3 to a final ca.  $2 \times 10^{-4}$  M concentration (inset indicates the decrease at 340 nm, 800 s). (b) Variation of the value of  $k_{\text{obs}}$  for the reaction indicated with pH at 35 °C.

**Table 2. Summary of the Kinetic and Thermal and Pressure Activation Parameters Determined for the Reaction Observed on Dilution in Water of a DMSO Solution of Complex  $[\text{Cu}(\text{cis-V-AMME-N}_3\text{S}_3\text{sar})]^{2+}$  According to Scheme 2**

pH	halide	$10^3 \times {}^{298}k/\text{s}^{-1}$	$\Delta H^\ddagger/\text{kJ mol}^{-1}$	$\Delta S^\ddagger/\text{J K}^{-1} \text{mol}^{-1}$	$\Delta V^\ddagger/\text{cm}^3 \text{mol}^{-1}$
3.0	none	2.6	$83 \pm 4$	$-16 \pm 12$	$-7.3 \pm 0.4$
3.0	$\text{Br}^-$ , 3 M	0.25	$92 \pm 5$	$-11 \pm 17$	$-3.0 \pm 0.2$
3.0	$\text{Cl}^-$ , 3 M	0.27	$99 \pm 5$	$15 \pm 18$	not measured
9.7	none	90	$59 \pm 4$	$-69 \pm 15$	not measured
9.7	$\text{Br}^-$ , 3 M	2.9	$83 \pm 6$	$-17 \pm 18$	not measured
9.7	$\text{Cl}^-$ , 3 M	2.7	$90 \pm 3$	$-6 \pm 10$	not measured

centers capable of acting as hydrogen bonding donors and acceptors, respectively, supports this assumption.

**Absence of the “Cu(II)-out” Species in Aqueous Solution.** Previously we identified a novel redox-triggered “Cu-in”/“Cu-out” movement of the complex  $[\text{Cu}(\text{cis-V-AMME-N}_3\text{S}_3\text{sar})]^{2+}$  in DMSO solution using cyclic voltammetry.<sup>1</sup> We conducted a similar experiment here in water (Figure 7). A single cathodic ( $\text{Cu}^{\text{II}} \rightarrow \text{Cu}^{\text{I}}$ ) and single anodic ( $\text{Cu}^{\text{I}} \rightarrow \text{Cu}^{\text{II}}$ ) peak were observed but at very different potentials. The peak potentials were independent of sweep rate up to 500 mV/s. Successive cycles also gave no change with time.

The cathodic sweep shows only a single peak at ca.  $-375$  mV (versus Ag/AgCl) while a single anodic peak appears at  $-120$  mV. The wide separation indicates that (reversible) chemical reactions are coupled to electron transfer. On the basis of our spectroscopic data, the initial reduction process involves “Cu-in”  $[\text{Cu}(\text{cis-V-AMME-N}_3\text{S}_3\text{sar})]^{2+}$ , but the absence of a corresponding anodic peak at a similar potential indicates that the putative monovalent “Cu-in”  $[\text{Cu}(\text{cis-V-AMME-N}_3\text{S}_3\text{sar})]^{+}$  is unstable and rapidly rearranges to a form that is oxidized at a much higher potential (anodic peak at  $-120$  mV). By analogy with our observations in DMSO solution,<sup>1</sup> the higher potential oxidation wave is due to the tetradentate coordinated “Cu-out”  $[\text{Cu}(\text{AMME-N}_3\text{S}_3\text{sar})]^{+}$  form. An interesting contrast between water and DMSO<sup>1</sup> in this system is that oxidation of this “Cu-out”  $[\text{Cu}(\text{AMME-N}_3\text{S}_3\text{sar})]^{+}$  complex in water does not generate a stable “Cu-out” divalent  $[\text{Cu}(\text{AMME-N}_3\text{S}_3\text{sar})]^{2+}$  complex (with a corresponding high potential cathodic peak). Instead, rapid re-entry of the Cu(II) ion to the interior of the cage is apparent as the second cathodic sweep is identical to the first.

In this respect 1 mM solutions of  $[\text{Cu}(\text{cis-V-AMME-N}_3\text{S}_3\text{sar})](\text{ClO}_4)_2$  in water at pH 3.0 and with NaBr or NaCl up to 3 M showed no differences in their EPR spectra, thus indicating that no significant build up of the “Cu-out” complex (Scheme 2) occurs in aqueous media (Figure 8). Furthermore, simulation of the spectra (Figure S4) produced a set of  $g$  values

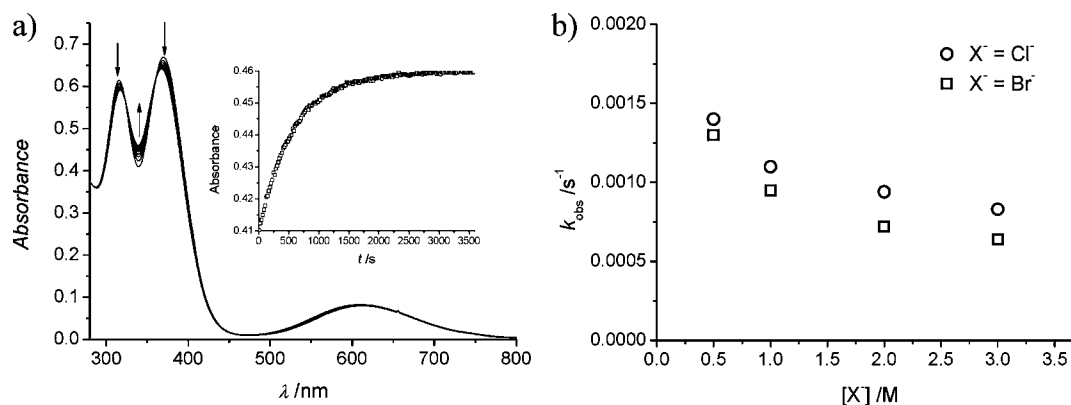


**Figure 5.** (a) Changes in the UV-vis spectra over time for the reaction of the  $[\text{Cu}(\text{cis-V-AMME-N}_3\text{S}_3\text{sar})]^{2+}$  complex with chloride in water ( $T = 35$  °C, pH 3,  $[\text{Cl}^-] = 0.5$  M,  $I = 3$  M  $\text{NaClO}_4$ ). The inset corresponds to the absorbance changes over time at 340 nm, total time 1 h. (b) Trends of the values of  $k_{\text{obs}}$  for the same reaction as a function of halide concentration at 35 °C and pH = 3.0.

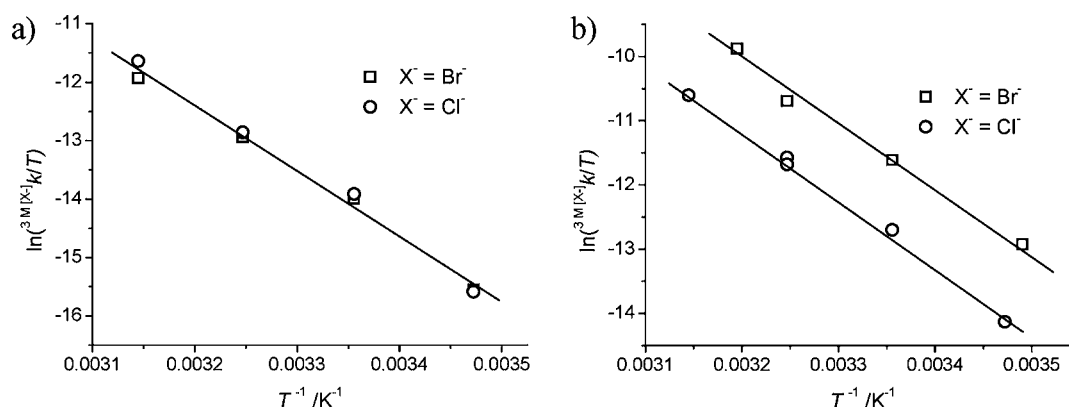


**Figure 6.** (a) Eyring plot for the value of  $k_{\text{obs}}$  for the process observed on reaction of 3 M halide solutions with a solution of  $[\text{Cu}(\text{cis-V-AMME-N}_3\text{S}_3\text{sar})]^{2+}$  in water at pH = 3.0. (b) Eyring plot for the value of  $k_{\text{obs}}$  for the process observed on reaction of 3 M halide solutions with a solution of  $[\text{Cu}(\text{cis-V-AMME-N}_3\text{S}_3\text{sar})]^{2+}$  in water at pH = 9.7.

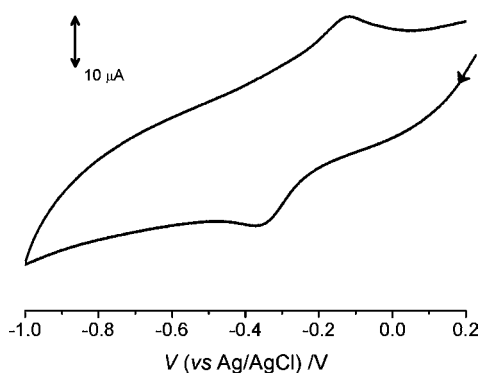


**Figure 7.** Cyclic voltammogram of a  $5 \times 10^{-4}$  M aqueous solution of  $[\text{Cu}(\text{cis-V-AMME-N}_3\text{S}_3\text{sar})]^{2+}$  in water at a sweep rate of 100 mV at a glassy carbon electrode and in 0.1 M  $\text{NaClO}_4$ .

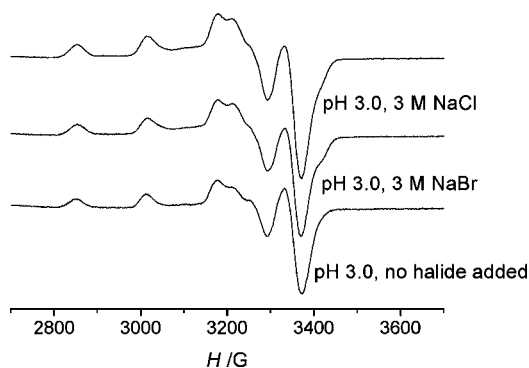


**Figure 8.** EPR spectra (9.3966 GHz) of frozen  $1 \times 10^{-3}$  M different aqueous solutions at pH 3.0 of  $[\text{Cu}(\text{cis-V-AMME-N}_3\text{S}_3\text{sar})](\text{ClO}_4)_2$  after 2 h of mixing.

that basically agree with those determined previously<sup>1</sup> for the  $[\text{Cu}(\text{cis-V-AMME-N}_3\text{S}_3\text{sar})](\text{ClO}_4)_2$  complex in DMSO solution.

## CONCLUSIONS

Summarizing, in nonaqueous solvents (DMSO and MeCN), a small amount of 5-coordinate “Cu-out” complex  $[\text{Cu}(\text{trans-II-AMME-N}_3\text{S}_3\text{sar})(\text{Solvent})]^{2+}$  (Scheme 2) is in equilibrium with the encapsulated “Cu-in” complex  $[\text{Cu}(\text{cis-V-AMME-N}_3\text{S}_3\text{sar})]^{2+}$ . In water, the equilibrium lies entirely to the left with the “Cu-in” complex  $[\text{Cu}(\text{cis-V-AMME-N}_3\text{S}_3\text{sar})]^{2+}$

(Scheme 2) the only detectable species. On dilution of DMSO or MeCN solutions of  $[\text{Cu}(\text{AMME-N}_3\text{S}_3\text{sar})]^{2+}$  in water, complete re-entry of the Cu ion back into the cage was observed. It is also clear that the formation of  $[\text{Cu}(\text{cis-V-AMME-N}_3\text{S}_3\text{sar})]^{2+}$  from  $[\text{Cu}(\text{trans-II-AMME-N}_3\text{S}_3\text{sar})(\text{OH}_2)]^{2+}$  in water is slower than the corresponding reaction in pure DMSO/MeCN and involves significant hydrogen bonding interactions in the transition state (negative  $\Delta V^\ddagger$  and practically zero  $\Delta S^\ddagger$ ). As a consequence, the amount of  $[\text{Cu}(\text{trans-II-AMME-N}_3\text{S}_3\text{sar})(\text{OH}_2)]^{2+}$  or its conjugate base in solution is minute, thus preventing the formation of significant amounts of  $[\text{Cu}(\text{trans-III-AMME-N}_3\text{S}_3\text{sar})(\text{X})]^+$  even at concentration of halides as high as 3 M. The fact that the Lewis basicities of both  $\text{Br}^-$  and  $\text{Cl}^-$  are greatly diminished going from the aprotic solvents DMSO and MeCN to water, where  $\text{H}-\text{O}-\text{H}\cdots\text{X}^-$  H-bonding to the halide ions competes with metal ion coordination, can also be determinant in the lack of “Cu-out” complexes observed in water. The stability of the completely encapsulated  $[\text{Cu}(\text{cis-V-AMME-N}_3\text{S}_3\text{sar})]^{2+}$  complex in water and its resistance to attack by halide ions (in contrast to its behavior in MeCN or DMSO) is important and bodes well for the application of complexes of this kind in  $^{64}\text{Cu}$  PET imaging<sup>14</sup> or other applications that demand a stable and robust Cu complex at neutral aqueous solution.

## EXPERIMENTAL SECTION

**Compounds.** 1-Methyl-8-amino-3,13,16-trithia-6,10,19-triazabicyclo[6.6.6]-eicosanecopper(II) perchlorate,  $[\text{Cu}(\text{AMME-N}_3\text{S}_3\text{sar})](\text{ClO}_4)_2$ , was prepared as described.<sup>1</sup> Halide ions were added as  $(\text{Bu}_4\text{P})\text{X}$  in DMSO and MeCN solutions, or as  $\text{NaX}$  in aqueous medium.

**Kinetic Measurements.** For reactions at atmospheric pressure with  $t_{1/2} > 30$  s, kinetic runs were recorded with Cary50 or HP8453 instruments, equipped with a thermostatted multicell holder; for runs with shorter half-life times a stopped-flow mixing unit from Applied Photophysics connected with fiber optics to a TIDAS instrument was used. For experiments run at variable pressure a previously described setup was used.<sup>15,17,23</sup>

All halide association reactions were carried out under pseudo-first-order conditions ( $[\text{X}^-]/[\text{Cu}^{II}] > 10$ ) in DMSO or MeCN as solvents and with the ionic strength kept constant at 0.17 M with  $\text{NaClO}_4$  unless stated. For the rest of the experiments neat solvent (unless stated) was used with the pH buffered in water. Standard non-coordinating buffers<sup>35</sup> and PIPPS<sup>36</sup> (pH 3) were used for this purpose. The concentrations of the copper complex were in the range  $(1-4) \times 10^{-4}$  M generally; the general kinetic procedure has been already described.<sup>1</sup> The program Specfit<sup>37</sup> was used for data manipulation and

analysis, and observed rate constants were derived from the absorbance versus time traces at wavelengths where a maximum change in absorbance was observed. Tables S1 and S2 in the Supporting Information collect all the values obtained for  $k_{\text{obs}}$  for the different reaction studied and under the specified conditions.

**Physical Methods.** Cyclic voltammetry was performed with a BioLogic potentiostat employing a glassy carbon working electrode, platinum auxiliary electrode, and Ag/AgCl reference electrode; 0.1 M NaClO<sub>4</sub> was the supporting electrolyte in all experiments. All solutions contained 0.5–1.0 mM concentrations of copper complex and were purged with nitrogen before measurement. Electron paramagnetic resonance (EPR) spectra were measured with a Bruker ESP300E instrument at X-band frequency ( $\nu = 9.3966$  GHz) at the Serveis Científics Tècnics de la Universitat de Barcelona as  $1 \times 10^{-3}$  M frozen DMSO or water solutions at 140 K, as indicated in the text.

## ■ ASSOCIATED CONTENT

### ■ Supporting Information

Additional figures and tables. This material is available free of charge via the Internet at <http://pubs.acs.org>.

## ■ AUTHOR INFORMATION

### Corresponding Author

\*E-mail: [p.bernhardt@uq.edu.au](mailto:p.bernhardt@uq.edu.au) (P.V.B.), [manel.martinez@qi.ub.edu](mailto:manel.martinez@qi.ub.edu) (M.M.).

### Notes

The authors declare no competing financial interest.

## ■ ACKNOWLEDGMENTS

Financial support from the Spanish Ministerio de Economía y Competitividad (CTQ2012-37821-CO2-01) and the Australian Research Council (DP1096029) is acknowledged.

## ■ REFERENCES

- (1) Bell, C. A.; Bernhardt, P. V.; Gahan, L. R.; Martínez, M.; Monteiro, M. J.; Rodríguez, C.; Sharrad, C. A. *Chem.—Eur. J.* **2010**, *16*, 3166–3175.
- (2) Grondhal, L. A.; Hammershoi, A.; Sargeson, A. M.; Thöm, V. J. *Inorg. Chem.* **1997**, *36*, 5396–5403.
- (3) Gahan, L. R.; Hambley, T. W.; Sargeson, A. M.; Snow, M. R. *Inorg. Chem.* **1982**, *21*, 2699–2706.
- (4) Geue, R. J.; Hambley, T. W.; Harrowfield, J. M.; Sargeson, A. M.; Snow, M. R. *J. Am. Chem. Soc.* **1984**, *106*, 5478–5488.
- (5) Bottomley, G. A.; Clark, I. J.; Creaser, I. I.; Engelhardt, L. M.; Geue, R. J.; Hagen, K. S.; Harrowfield, J. M.; Lawrance, G. A.; Lay, P. A.; Sargeson, A. M.; See, A. J.; Skelton, B. W.; White, A. H.; Wilner, F. R. *Aust. J. Chem.* **1994**, *47*, 143–179.
- (6) Gahan, L. R.; Donlevy, T. M.; Hambley, T. W. *Inorg. Chem.* **1990**, *29*, 1451–1454.
- (7) Powell, D. H.; Helm, L.; Merbach, A. E. *J. Chem. Phys.* **1991**, *95*, 9258.
- (8) Helm, L.; Lincoln, S. F.; Merbach, A. E.; Zbinden, D. *Inorg. Chem.* **1986**, *25*, 2550–2552.
- (9) Bernhardt, P. V.; Bramley, R.; Engelhardt, L. M.; Harrowfield, J. M.; Hockless, D. C. R.; Korybut-Daszkiewicz, B. R.; Krausz, E. R.; Morgan, T.; Sargeson, A. M. *Inorg. Chem.* **1995**, *34*, 3589–3599.
- (10) Qin, C. J.; James, L.; Chartres, J. D.; Alcock, L. J.; Davis, K. J.; Willis, A. C.; Sargeson, A. M.; Bernhardt, P. V.; Ralph, S. F. *Inorg. Chem.* **2011**, *50*, 9131–9140.
- (11) Bernhardt, P. V.; Bramley, R.; Geue, R. J.; Ralph, S. F.; Sargeson, A. M. *Dalton Trans.* **2007**, 1244–1249.
- (12) Engelhardt, L. M.; Harrowfield, J. M.; Harrowfield, J. M.; Ralph, S. F.; Sargeson, A. M.; Skelton, B. W.; Sobolev, A.; White, A. H. *J. Inclusion Phenom. Macrocyclic Chem.* **2011**, *71*, 353–362.
- (13) Bernhardt, P. V.; Harrowfield, J. M.; Hockless, D. C. R.; Sargeson, A. M. *Inorg. Chem.* **1994**, *33*, 5659–5670.

(14) Voss, S. D.; Smith, S. V.; DiBartolo, N.; McIntosh, L. J.; Cyr, E. M.; Bonab, A. A.; Dearling, J. L. J.; Carter, E. A.; Fischman, A. J.; Treves, S. T.; Gillies, S. D.; Sargeson, A. M.; Huston, J. S.; Packard, A. B. *Proc. Natl. Acad. Sci. U.S.A.* **2007**, *104*, 17489–17493.

(15) Aullón, G.; Bernhardt, P. V.; Bozoglián, F.; Font-Bardía, M.; Macpherson, B. P.; Martínez, M.; Rodríguez, C.; Solans, X. *Inorg. Chem.* **2006**, *45*, 8551–8562.

(16) Bernhardt, P. V.; Martínez, M.; Rodríguez, C. *Inorg. Chem.* **2009**, *48*, 4787–4797.

(17) Bernhardt, P. V.; Martínez, M.; Rodríguez, C.; Vazquez, M. *Inorg. Chem.* **2011**, *50*, 1429–1440.

(18) Lawrance, G. A.; Martínez, M.; Skelton, B. W.; White, A. H. *Aust. J. Chem.* **1991**, *44*, 113–121.

(19) Lawrance, G. A.; Manning, T. M.; Maeder, M.; Martínez, M.; O’Leary, M. A.; Patalinghug, W.; Skelton, A. W.; White, A. G. *J. Chem. Soc., Dalton Trans.* **1992**, 1635–1641.

(20) Basallote, M. G.; Castillo, C. E.; Lubal, P.; Mañez, M. A.; Martínez, M.; Rodríguez, C.; Vanek, J. *Inorg. Chem. Commun.* **2010**, *12*, 1272–1274.

(21) Calvet, T.; Crespo, M.; Font-Bardía, M.; Jansat, S.; Martínez, M. *Organometallics* **2012**, *31*, 4367–4373.

(22) Aullón, G.; Jansat, S.; Gómez, K.; González, G.; Martínez, M.; Poli, R.; Rodríguez-Zubiri, M. *Inorg. Chem.* **2011**, *50*, 5628–5636.

(23) Aviles, T.; Jansat, S.; Martínez, M.; Montilla, F.; Rodríguez, C. *Organometallics* **2011**, *30*, 3919–3922.

(24) Aullón, G.; Chat, R.; Favier, I.; Font-Bardía, M.; Gómez, M.; Granell, J.; Martínez, M.; Solans, X. *Dalton Trans.* **2009**, 8292–8300.

(25) Favier, I.; Gómez, M.; Granell, J.; Martínez, M.; Font-Bardía, M.; Solans, X. *Dalton Trans.* **2005**, 123–132.

(26) Granell, J.; Martínez, M. *Dalton Trans.* **2012**, *41*, 11243–11258.

(27) Bosnich, B.; Poon, C. K.; Tobe, M. L. *Inorg. Chem.* **1965**, *4*, 1102–1108.

(28) Espenson, J. H. *Chemical Kinetics and Reaction Mechanisms*; McGraw-Hill: New York, 1981.

(29) Martínez, M.; Pitarque, M. A.; van Eldik, R. *J. Chem. Soc., Dalton Trans.* **1996**, 2665–2671.

(30) Martínez, M.; Pitarque, M. A.; van Eldik, R. *Inorg. Chim. Acta* **1997**, *256*, 51–59.

(31) Bernhardt, P. V.; Bozoglián, F.; Macpherson, B. P.; Martínez, M.; González, G.; Sierra, B. *Eur. J. Inorg. Chem.* **2003**, 2512–2518.

(32) Otto, R.; Brox, J.; Trippel, S.; Stei, M.; Best, T.; Wester, R. *Nat. Chem.* **2012**, *4*, 534–538.

(33) Bernhardt, P. V.; Gallego, C.; Martínez, M.; Parella, T. *Inorg. Chem.* **2002**, *41*, 1747–1754.

(34) Gallego, C.; González, G.; Martínez, M.; Merbach, A. E. *Organometallics* **2004**, *23*, 2434–2438.

(35) Perrin, D. D. *Aust. J. Chem.* **1963**, *16*, 572–578.

(36) Bernhardt, P. V.; Martínez, M.; Rodríguez, C.; Vazquez, M. *Dalton Trans.* **2012**, *41*, 2122–2130.

(37) Binstead, R. A.; Zuberbuhler, A. D.; Jung, B. *SPECFIT32* [3.0.34]; Spectrum Software Associates: Singapore, 2005.